**Aalborg Universitet**

**AALBORG UNIVERSITY**
DENMARK

**Energy management and optimization of vehicle-to-grid systems for wind power integration**

Wang, Wei; Liu, Liu; Liu, Jizhen; Chen, Zhe

# Energy Management and Optimization of Vehicle-to-grid Systems for Wind Power Integration

Wei Wang, Liu Liu, Jizhen Liu, and Zhe Chen, *Fellow, IEEE*

*Abstract*—An approach to smoothing the fluctuations of large-scale wind power is investigated using vehicle-to-grid (V2G) systems. First, an energy management and optimization system is designed and modeled. By using the wavelet packet decomposition method, the target grid-connected wind power, the required electric vehicle (EV) power, and supercapacitor power are determined. The energy management model for EVs is then developed by introducing a knapsack problem that can evaluate the needs of an EV fleet. Furthermore, an optimized dispatch strategy for EVs and wind power is developed by using a dynamic programming method. A case study demonstrates that the energy management and optimization method for V2G systems achieves noticeable performance improvements over benchmark techniques.

*Index Terms*—Dynamic programming, electric vehicle, knapsack problem, wavelet packet decomposition, wind power integration.

## NOMENCLATURE

| | |
|---|---|
| $P_{wind}$ | Original wind power output. |
| $P_w$ | Wind power excluding wind curtailment. |
| $P_{cur}$ | Wind curtailment power. |
| $P_{HESS}$ | HESS power output. |
| $P_{grid}$ | Target grid-connected power. |
| $P_{EV}$ | Output power of EV cluster. |
| $P_{SC}$ | Output power of SC. |
| $\Delta P$ | Target smoothing power deviations. |
| $\Delta P_{grid,1\,min}$ | Differences between the maximum and minimum power values in 1 min. |
| $\Delta P_{grid,10\,min}$ | Differences between the maximum and minimum power values in 10 min. |
| $P_{wind,ins}$ | Installed capacity of the wind farm. |
| $S$ | EV SOC. |
| $t_{arr}$ | EV arrival time. |
| $t_{dep}$ | EV departure time. |
| $S_{arr}$ | SOC value when EV arriving. |
| $S_{dep}$ | SOC value when EV departing. |
| $t$ | Sample time. |
| $h$ | Sample interval. |
| $P_c$ | EV charging power. |
| $P_d$ | EV discharging power. |
| $\eta_{EV}$ | EV operation efficiency. |
| $\eta_c$ | EV charging efficiency. |
| $\eta_d$ | EV discharging efficiency. |
| $E_{rated}$ | EV rated storage capacity. |
| $T_{c2d}$ | Required minimum time interval from charging to discharging. |
| $T_{d2c}$ | Required minimum time interval from discharging to charging. |
| $cou_{c2d}$ and $cou_{d2c}$ | Counts of two kinds of state changes, charging to discharging and discharging to charging. |
| $E_c$ | Maximum charging potential. |
| $E_d$ | Maximum discharging potential. |
| $t_{dis,max}$ | Time of EV reaching maximum discharge level. |
| $N_{EV}$ | Number of dispatchable EVs. |
| $N_f$ | Number of forced charging EVs. |
| $S_{SC}$ | SOC value of SC. |
| $E_{SC,rated}$ | SC rated energy storage capacity. |
| $P_{SC,c}$ | SC charging power. |
| $P_{SC,d}$ | SC discharging power. |
| $P_{SC,c,rated}$ | SC rated charging power. |
| $P_{SC,d,rated}$ | SC rated discharging power. |
| $\eta_{SC,c}$ | SC charging efficiency. |
| $\eta_{SC,d}$ | SC discharging efficiency. |
| $N_{SC,c}$ | Number of SC in charging state. |
| $N_{SC,d}$ | Number of SC in discharging state. |
| $c_i$ | Value of EV $i$. |
| $Ecd$ | EV maximum dispatch potential. |
| $T_{rem}$ | Remaining time in the power grid. |
| $\alpha$, $\beta$ and $\gamma$ | Weight coefficients. |

## SUBSCRIPTS

| | |
|---|---|
| $i$ | Index of EV. |
| max | Maximum value. |
| min | Minimum value. |

W. Wang (corresponding author, email: wwang@ncepu.edu.cn; ORCID: https://orcid.org/0000-0003-3952-2861) and J. Liu are with the State Key Laboratory of Alternate Electrical Power System with Renewable Energy Sources, North China Electric Power University, Beijing 102206, China.

L. Liu is with the School of Control and Computer Engineering, North China Electric Power University, Beijing 102206, China.

Z. Chen is with the Department of Energy Technology, Aalborg University, 9220 Aalborg, Denmark.

## I. INTRODUCTION

IN recent years, the scale of global renewable energy power, especially for wind power, has rapidly expanded under the background of ecological deterioration and the lack of

fossil energy [1]. However, the randomness, intermittent and uncertainty seriously affects the reliability of the power system and causes a great deal of problems when connected to the power grid. So, grid-connected power is required to be within certain limits to ensure the safety and stability of the power system [2], [3]. And it has become a great challenge to improve the penetration rate of wind power generation in the power system [4].

Existing studies have shown that the applications of energy storage technology provide great help for the integration of fluctuant renewable energies [5]–[7]. And issues, such as the acquisition of target grid-connected power, the energy storage equipment selection, the energy storage capacity configuration method, and the control of energy storage equipment, have been widely studied. For the target grid-connected power acquisition, wavelet packet decomposition (WPD) based methods are commonly utilized due to their advantages on multi-scale decomposition and frequency band division in the signal, and have been proven through good performance [8]–[10]. As for the energy equipment selection, an active battery super-capacitor (SC) hybrid energy storage system (HESS) [11]–[13] has been put into use for assisting renewable energy grid connections due to their complementary characteristics: a battery has a relatively high energy density but a low power density, whereas an SC has a relatively high power density but a low energy density [14].

In order to reduce the investment costs of energy storage, electric vehicles (EVs), as energy storage components, are gradually being considered to replace battery cells [15], [16]. And its operability is becoming more and more satisfactory with the increasing number of EVs [17]–[19]. However, the mobility and uncertainty of EVs make their dispatch modes and methods quite different from the traditional battery when participating in smoothing the fluctuations of renewable energies [20], [21]. A highly comprehensive energy storage model for EVs, that can calculate the output power of each EV with high accuracy, is examined in [22]. A novel integrated framework of EVs and wind farms (WEV) is proposed in [23] to use the EVs charging and discharging to smooth the wind power penalty costs that are caused by overestimating and underestimating available wind power. In the meantime, a new multi-objective dynamic economic emission dispatching model based on the WEV system is developed to consider both emission and total cost objectives. A dispatch model considering several conflicting and competing objectives, such as providing vehicle-to-grid (V2G) service or coordinating with wind power, is presented in [24]. A HESS model containing EVs is built, and its comprehensive energy management method is analyzed in [25]. Subsequently, various strategies for EVs supporting renewable energy integration are developed on the basis of advanced smart metering and communication infrastructure [26], [27].

However, the problem still remains of how to dispatch and control the power output of EVs in the grid as the dynamic selection of optimal EV clusters for scheduling are a typical non-deterministic polynomial (NP) hard problem [28]. And there are still several bottleneck problems which have to be urgently determined [29]–[31]. First, the energy storage model of each EV varies because of its uncertainties. Second, the dynamic changes in the EV clusters in the grid and the real-time status of each EV are hard to evaluate. Third, EV clusters fail to maximize the suppression of power fluctuations, based on the fact that EV power dispatch simply follows the waiting principle without allocating power according to the optimal state of each EV. In addition to NP, the knapsack problem (KP) is also taken to describe the operational optimization problem of EVs in power systems with high wind power penetrations, where the goal is to maximize the total value of the items in the knapsack under some constraint conditions [32]. A dynamic programming (DP) algorithm is commonly employed to solve such problems, and it has been proved that DP algorithms can deal with KP remarkably well in high and low dimensions with different correlations [33], [34].

This study proposes a collaborative optimal dispatch method of vehicle-to-grid (V2G) systems for wind power integration. An appropriate DP algorithm is applied to determine the optimal scheduling of EV clusters, thereby making the energy exchange between EVs and the grid to work with high flexibility and efficiency. The proposed method also takes advantage of the hybrid energy storage technology and WPD method. The methods presented in this paper are briefly summarized as follows:

1) A highly accurate hybrid energy storage structure, especially for a single EV, is established in this study. The EV model becomes more complete by adding the constraint of charging and discharging times and the parking status in the scheduling process. The WPD method is used to calculate the target grid-connected power, and the total demand of EVs is estimated by removing the highest frequency layer of the decomposition result.

2) SCs are added and a new scheduling method that can use DP to determine the optimal scheduling cluster is designed, because of the unique characteristics of EVs. Through verification, we determined that the aforementioned method can make the wind power output as accurate as possible to the target grid-connected power calculated by WPD.

The paper is organized as follows. Section II formulates a detailed model of the wind storage hybrid system, which includes EV and SC energy storage models. Section III applies a V2G system dispatch method based on a DP algorithm. Section IV presents a case study to evaluate the proposed method. Section V presents the conclusion.

## II. STRUCTURAL MODEL AND OPERATING MODE OF HESS

### A. HESS Structure

HESS, in this paper, contains EV clusters and SC. If EVs cannot completely suppress the wind power fluctuations, an SC will be applied for replenishment. Also, a small amount of wind curtailment is allowable in this system. The overall structure of HESS for wind power integration is shown in Fig. 1.

The HESS operating mechanism is presented as follows:

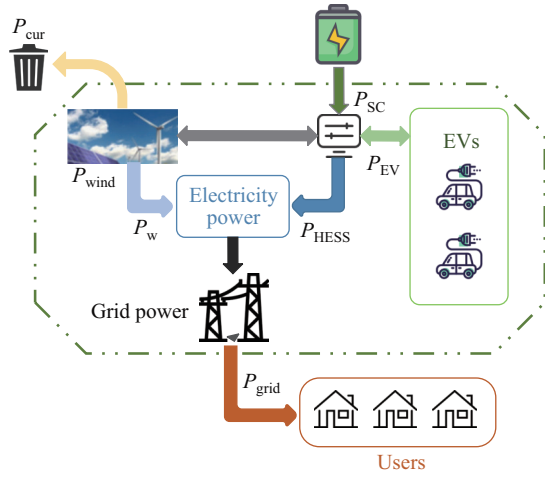$$P_{\text{w}}(t) + P_{\text{cur}}(t) = P_{\text{wind}}(t), \tag{1}$$

Fig. 1.   HESS structure.



Fig. 2.   Single EV energy storage model.

$$P_{\text{w}}(t) + P_{\text{HESS}}(t) = P_{\text{grid}}(t), \tag{2}$$

$$P_{\text{HESS}}(t) = P_{\text{EV}}(t) + P_{\text{SC}}(t), \tag{3}$$

$$\Delta P(t) = P_{\text{wind}}(t) - P_{\text{grid}}(t), \tag{4}$$

where $P_{\text{wind}}$ is the original wind power output; $P_{\text{w}}$ is the wind power excluding wind curtailment; $P_{\text{cur}}$ is the wind curtailment power; $P_{\text{HESS}}$ is the HESS power output; $P_{\text{grid}}$ is the target grid-connected power; $P_{\text{EV}}$ and $P_{\text{SC}}$ are the output power of the EV cluster and the supercapacitor, respectively; $\Delta P$ is the target smoothing power deviations.

In order to maintain the power system stability, the wind power is required to meet the grid-connected wind power fluctuation rate standard [35]. Regarding a wind farm with the installed capacity of 30–150 MW, its active power fluctuation requirements for the time scale of 1 min and 10 min is specified as follows:

$$\begin{cases} \Delta P_{\text{grid},1\,\text{min}} \leqslant \dfrac{P_{\text{wind,ins}}}{10}, \\ \Delta P_{\text{grid},10\,\text{min}} \leqslant \dfrac{P_{\text{wind,ins}}}{3}, \end{cases} \tag{5}$$

where $\Delta P_{\text{grid},1\,\text{min}}$ and $\Delta P_{\text{grid},10\,\text{min}}$ are the differences between the maximum and minimum power values in 1 min and 10 min, respectively; $P_{\text{wind, ins}}$ is the installed capacity of the wind farm.

*B. HESS Model*

In the HESS, EVs and SC will cooperate to smooth the fluctuations of wind power. Their operating mechanism and models are presented as follows:

*1) EV Model*

An EV is applied as an energy storage element to participate in power dispatch for wind power smoothing. When EVs are connected to the grid, power dispatch can be carried out under the constraints of the required state of charge (SOC), including the demanded SOC value of users, and charging and discharging time limits.

The operating mechanism and model for an EV is shown in Fig. 2, which describes the SOC variations during the charge or discharge process. The $Y$-axis ($S$) denotes the SOC value
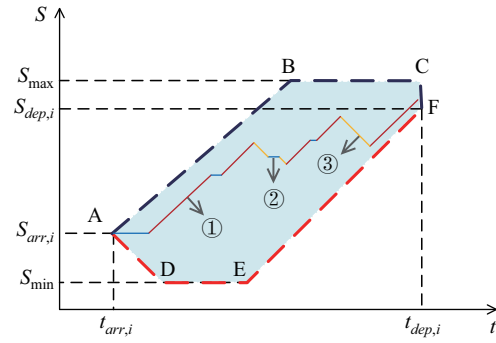
of an EV. The values of $S_{\text{min}}$ and $S_{\text{max}}$ are the minimum and maximum allowable SOC limitations where an EV is participating in power dispatch, respectively. $t_{\text{arr}}$ to $t_{\text{dep}}$ is the length of time of EVs to arrive at and depart from the grid, respectively. $S_{\text{arr}}$ is the initial SOC value when plugging into the power system. $S_{\text{dep}}$ is the demanded SOC value of users. A-B-C refers to the maximum boundary value of the SOC when an EV participates in dispatching, indicating that the EV is charged immediately after plugging into the grid. When the SOC reaches $S_{\text{max}}$, EV charging is finished, and the remaining time of SOC remains unchanged. D-E-F refers to the minimum boundary value of the SOC, indicating that the EV is discharged immediately. The discharge cannot be continued when the SOC value drops to $S_{\text{min}}$. If the EV remains in the grid for a long time, it can remain as not being charged. When the time reaches the mandatory charging time, the battery is recharged to ensure the travel demand of users. In Fig. 2, EF indicates the forced charging process.

The solid line in Fig. 2 shows a feasible power dispatching curve for EV $i$. Process ① represents the dispatching action of the EV for charging. Process ② represents that the EV is in a parked state without charging or discharging. Process ③ represents the dispatching action of the EV for discharge.

Suppose the sample time is $t$ and the sample interval is $h$, we can describe the EV state through the charge-discharge model of an EV as:

$$S_i(t) = S_i(t-1) + h\frac{P_{\text{EV},i}(t)\eta_{\text{EV},i}}{E_{\text{rated}}}, \tag{6}$$

$$P_{\text{EV},i}(t) = \begin{cases} P_{\text{c}} & P_{\text{EV},i}(t) > 0 \\ 0 & P_{\text{EV},i}(t) = 0 \,, \\ P_{\text{d}} & P_{\text{EV},i}(t) < 0 \end{cases} \tag{7}$$

$$\eta_{\text{EV},i}(t) = \begin{cases} \eta_{\text{c}} & P_{\text{EV},i}(t) > 0 \\ 0 & P_{\text{EV},i}(t) = 0 \\ 1/\eta_{\text{d}} & P_{\text{EV},i}(t) < 0 \end{cases} \tag{8}$$

where subscript $i$ is the EV number; $P_{\text{c}}$ and $P_{\text{d}}$ are the EV charging and discharging power, respectively; $\eta_{\text{EV}}$ is the EV operational efficiency; $\eta_{\text{c}}$ and $\eta_{\text{d}}$ are the EV charging and discharging efficiency, respectively; $E_{\text{rated}}$ is the EV rated storage capacity.

The constraints of an EV participating in energy storage

power dispatch are as follows:

$$S_{\min} \leqslant S_i(t) \leqslant S_{\max}, \tag{9}$$

$$t_{\text{arr},i} \leqslant t \leqslant t_{\text{dep},i}, \tag{10}$$

$$S_i(t) + P_c \eta_c (t_{\text{dep},i} - t)/E_{\text{rated}} - S_{\text{dep},i} \geqslant 0, \tag{11}$$

$$\sum_{t}^{t+T_{c2d}} cou_{c2d,i}(t) = 0, \tag{12}$$

$$\sum_{t}^{t+T_{d2c}} cou_{d2c,i}(t) = 0, \tag{13}$$

where Eq. (11) denotes that a schedulable EV is required to maintain its SOC value meeting the demand of users when it is off-grid; $T_{c2d}$ represents the required minimum time interval from charging to discharging; $T_{d2c}$ represents the required minimum time interval from discharging to charging; $cou_{c2d}$ and $cou_{d2c}$ are the counts of two types of state changes, i.e., from charging to discharging and from discharging to charging, respectively.

According to Eqs. (9)–(11), the maximum power dispatching potential of EV $i$ under constraint conditions can be described by:

$$E_{c,i}(t) = E_{\text{rated}}(S_{\max,i} - S_i(t))$$
$$s.t. \quad \begin{cases} S_{\max,i} \leqslant 1 \\ S_{\max,i} \leqslant S_i(t) + P_c \eta_c (t_{\text{dep},i} - t)/E_{\text{rated}} \end{cases} \tag{14}$$

$$E_{d,i}(t) = E_{\text{rated}}(S_i(t) - S_{\min,i})$$
$$s.t. \quad \begin{cases} S_{\min,i} = S_{\text{dep},i} - P_c \eta_c (t_{\text{dep},i} - t_{\text{dis,max}})/E_{\text{rated}} \\ S_{\min,i} = S_i(t) - P_d/\eta_d (t_{\text{dis,max}} - t)/E_{\text{rated}} \end{cases} \tag{15}$$

where $E_c$ and $E_d$ are the maximum charging and discharging potential, respectively; $t_{\text{dis,max}}$ denotes the time of the EV reaching maximum discharge level.

Commonly, the total number of EVs in a system is assured, but the number of EVs in the grid varies at each time point based on their randomness. Suppose the number of dispatchable EVs is $N_{\text{EV}}$, the accumulated power for EV cluster is $P_{\text{EV}}$, and the number of forced charging EV is $N_f$, we will have:

$$P_{\text{EV}}(t) = \sum_{i=1}^{N_{\text{EV}}} P_{\text{EV},i}(t). \tag{16}$$

If the dispatching EVs are taking the action of discharging,

$$P_{\text{EV}}(t) = \sum_{i=1}^{N_{\text{EV}}-N_f} P_{\text{EV},i}(t) + \sum_{i=1}^{N_f} P_{c,i}(t). \tag{17}$$

*2) SC Model*

The primary energy storage device in this study is the EV battery. In addition, the EV cluster, and SC are employed in this study to smooth the fluctuations which EVs cannot totally eliminate on account of their mobility and uncertainty. Referring to the EV model, the SOC of SC can be described by:

$$S_{\text{SC}}(t) = S_{\text{SC}}(t-1)+$$

$$h\frac{P_{\text{SC, c}}(t)\eta_{\text{SC, c}}}{E_{\text{SC, rated}}} N_{\text{SC, c}} - h\frac{P_{\text{SC, d}}(t)/\eta_{\text{SC, d}}}{E_{\text{SC, rated}}} N_{\text{SC, d}} \tag{18}$$

Operating constraints of SC are presented as follows:

$$S_{\text{SC,min}} \leqslant S_{\text{SC}}(t) \leqslant S_{\text{SC,max}}, \tag{19}$$

$$0 \leqslant P_{\text{SC, c}}(t) \leqslant P_{\text{SC, c, rated}}, \tag{20}$$

$$P_{\text{SC, d, rated}} \leqslant -P_{\text{SC, d}}(t) \leqslant 0, \tag{21}$$

$$0 \leqslant N_{\text{SC, c}}(t) + N_{\text{SC, d}}(t) \leqslant 1, \tag{22}$$

where $S_{\text{SC}}$ denotes the SOC value of SC, $E_{\text{SC, rated}}$ is the SC rated energy storage capacity, $S_{\text{SC,min}}$ and $S_{\text{SC,max}}$ are the SOC limits of SC; $P_{\text{SC, c}}$ and $P_{\text{SC, d}}$ are the SC charging and discharging powers, respectively; $P_{\text{SC, c, rated}}$ and $P_{\text{SC, d, rated}}$ are the SC rated charging and discharging powers, respectively; $\eta_{\text{SC, c}}$ and $\eta_{\text{SC, d}}$ are the SC charging and discharging efficiencies, respectively; $N_{\text{SC, c}}$ and $N_{\text{SC, d}}$ represent the number of SCs in the charging and discharging states, respectively.

*C. HESS Power Distribution Based on WPD*

The WPD algorithm adopted in this study is a new signal analysis method based on wavelet analysis. It not only allows for the defect of wavelet analysis which cannot decompose high-frequency parts, but also it can select the frequency band which matches the signal spectrum. Through WPD algorithm [36], the target grid-connected wind power, together with the HESS power distribution, can be obtained. The schematic of the WPD method is shown in Fig. 3.
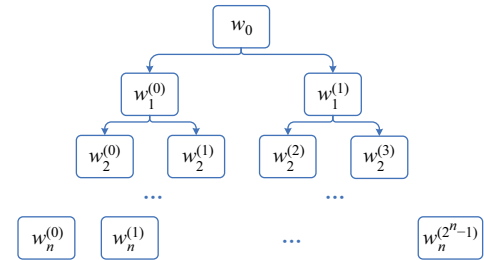


Fig. 3. Schematic of WPD.

Given the orthogonal scaling function $\Phi(x)$ and wavelet function $\Psi(x)$, the scale relationship is presented as follows:

$$\Phi(x) = \sum_{k \in Z} h_{0k} \Phi(2x - y), \tag{23}$$

$$\Psi(x) = \sum_{k \in Z} h_{1k} \Phi(2x - y). \tag{24}$$

$$w_n^{(2j)}(x) = \sqrt{2} \sum_{k \in Z} h_{0k} w_n^{(j)}(2x - y), \tag{25}$$

$$w_n^{(2j+1)}(x) = \sqrt{2} \sum_{k \in Z} h_{1k} w_n^{(j)}(2x - y), \tag{26}$$

where $h_{0k}$ and $h_{1k}$ are the filters in the multiresolution analysis, $n$ is the number of WPD layers (or the number of oscillations), $n \in Z$, and $n = 0$ means the signal has not been decomposed. $y$ is the position index, and $j$ is the scale index.

The first branch of WPD has the largest energy proportion and the lowest frequency in the original signal. This part is selected as the target grid-connected power in this study. The last branch is the highest frequency portion of the original

signal, which is mitigated by energy storage elements that are sensitive to frequency changes, such as SCs. The sum from the branch of $w_n^{(1)}(x)$ to $w_n^{(2^{n-1}-2)}(x)$ is used to select the amount of EVs.

## III. DISPATCH MODEL AND APPROACH

### A. Dispatch Model

To take full advantage of V2G systems and increase the penetration rate of wind power in the power grid, we propose a new scheduling model based on the balance between supply and demand. The specific model is developed as follows:

1) Target grid-connected power and target smoothing deviation are calculated on the basis of WPD.
2) The total amount of EVs in the region that can be dispatched and the travel parameters of users are confirmed. The dispatchable capacities of the EVs are evaluated.
3) Charging and discharging strategies are selected on the basis of the demand for smooth deviation.
   a) When $\Delta P(t) > 0$, dispatching action is selected for charging, and the demand for the EV numbers is determined as $N_r(t)$. According to the real-time status of EVs, $N_{EV}(t)$ can be obtained.
   b) When $\Delta P(t) < 0$, $N_r(t)$ and $N_{EV}(t)$ can be obtained. The forced charging EVs do not discharge in this case.
4) The EV cluster that participates in dispatching is determined on the basis of the supply and demand balance.
   a) When $N_{EV}(t) \leqslant N_r(t)$, the supply cannot meet the demand or meet the demand exactly. All EVs that can participate in power dispatching will be operated at this moment.
   b) When $N_{EV}(t) > N_r(t)$, the supply can meet the demand, and a surplus exists. KP-based DP is called to seek the optimal strategy, and the number of the optimal dispatch EVs $N_{opt}(t)$ will be obtained.
5) The real-time output power of the EV cluster is calculated. The SC is added for replenishment when the target deviation power cannot be suppressed as expected.
6) The next power dispatch action proceeds until the end of the calculation cycle.

The specific scheduling flow chart is shown in Fig. 4.

### B. 01 KP Description

The KP is a typical NP-hard problem. It refers to some items that can only be taken or not be taken, each of them has a corresponding weight and value. There is a knapsack with a certain capacity, the requirement is to take a portion of some of the items. This portion is sufficient to fill the knapsack and maximize the total value of the items in the knapsack. To apply the KP algorithm to the EV cluster power dispatch, we define the value of each EV at time $t$ as:

$$c_i(t) = -\alpha cou_i(t) + \beta E_{cd,i}(t) + \gamma T_{rem,i}, \quad (27)$$

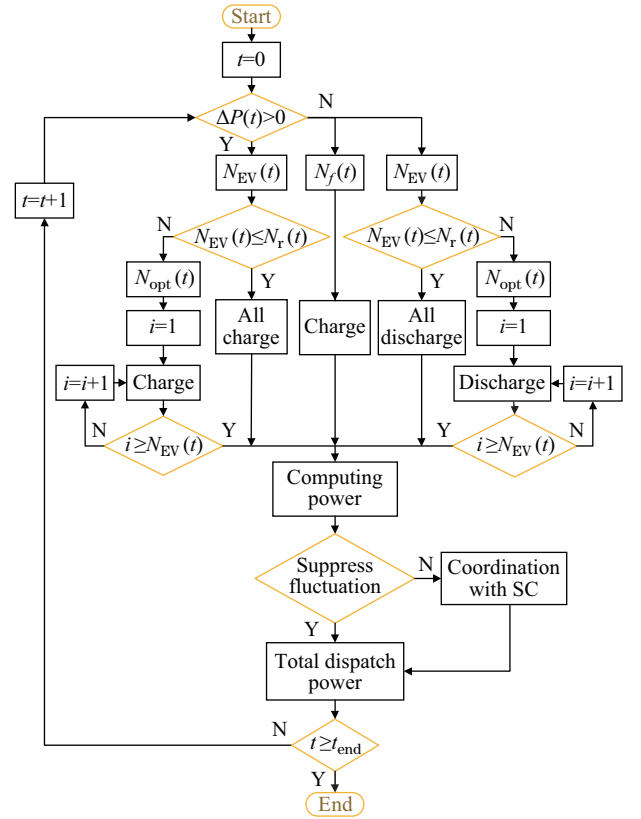$$cou_i(t) = \sum_{t_{arr}}^{t} (cou_{c2d,i}(t) + cou_{d2c,i}(t)), \quad (28)$$



Fig. 4.　Specific scheduling flow chart for dispatch.

$$E_{cd,i}(t) = \begin{cases} E_{c,i}(t) & P(t) \geqslant 0 \\ E_{d,i}(t) & P(t) < 0 \end{cases}, \quad (29)$$

where $c_i$ is the value of EV $i$; $E_{cd}$ is the EV maximum dispatch potential; $T_{rem}$ is the remaining time in the power grid, $\alpha$, $\beta$ and $\gamma$ are the weight coefficients.

The objective function is expressed as follows:

$$\begin{aligned} \max f &= \sum_{i \leqslant N_{opt}(t)} c_i(t) \\ \text{s.t.} \quad P_e(t) &= \sum_{i \leqslant N_{opt}(t)} P_{c,d}(t) \end{aligned} \quad (30)$$

where $f$ is the total value of EVs.

### C. DP Method

DP is a mathematical method used to solve the optimization of a multistage decision process. Dynamic means that the decisions of each period are determined by the development of a time process. The time factor can be introduced artificially when dealing with static problems. DP can also be transformed into a multistage decision problem, in which the decision process is divided into several interrelated stages, and each stage corresponds to a group of alternative decisions. The selection of each decision not only depends on the current situation but also affects the overall control effect in the future.

In this study, the problem can be converted into a strategy to find the optimal dispatching result of EVs when the demand for EVs is greater than the demand at $t$. The specific solution method is presented as follows:

1) Segmentation Problem: $i_{th}$ dispatches $i_{th}$ EV into the "knapsack."

2) State Variables $w_i^K$: the residual capacity of the knapsack for $i_{th}$ EV dispatching.

3) Decision Variables $D_i$: a decision on whether to dispatch EV $i$ for $i_{th}$ is made; yes is 1; otherwise, 0.

4) Transition Equation

$$f\left[i, w_i^K\right] = \max$$

$$\left\{ f\left[i-1, w_{i-1}^K\right] + c_i(w_i^K \geqslant w_i^{EV}), f(i-1, w_i^K) \right\}. \quad (31)$$

5) Optimal Power Dispatch EV Cluster $N_{opt}$.

## IV. CASE STUDY

### A. Results of Wind Power Analysis by WPD

Taking the data of a characteristic day of a wind power plant as an example, the rated power is 50 MW. The sampling period is set as 10 s, the sampling points are set as 8,640, and the total length of time is set as 24 h.

The target grid-connected power signal $P_{grid}(t)$ is calculated through the WPD algorithm. The minimum WPD layer in this case is 5. When $n = 5$, the first branch of WPD can satisfy the constraint of power grid incorporation. Fig. 5 shows that the original output power has strong fluctuation, whereas the grid-connected wind power is smoother. Fig. 6 shows the partial graph of the first branch of different decomposition WPD layers and the point where it does not meet the grid-connected power constraint. When WPD is not carried out ($n = 0$), the over-limit situation becomes worse. With the increase in the number of decomposition layers, the over-limit condition decreases significantly until $n = 5$ is completely satisfied.
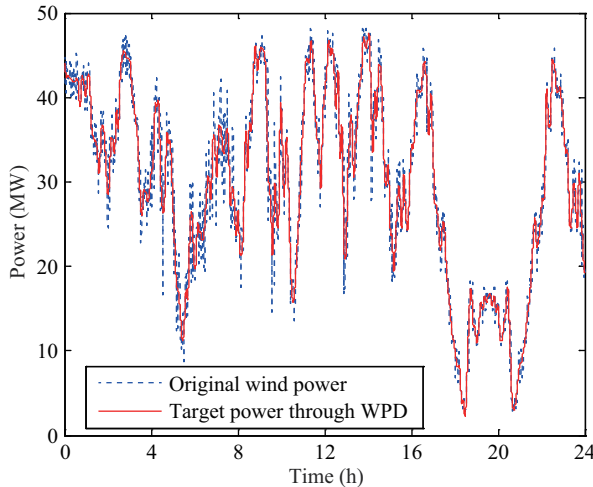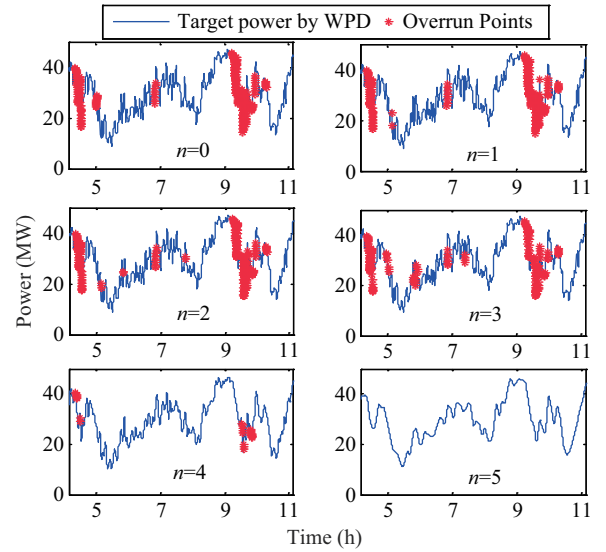


Fig. 6. Target grid-connected wind power and the overrun points in different WPD layers.

and the charging and discharging efficiency is at 90%. When EVs are in dispatch action for charging, no change from charging to discharging occurs within 1.5 hours. When EVs are in dispatch action for discharge, no change from discharging to charging occurs within 1 hour (except when there is forced charging). When the SOC of EVs is greater than 0.4, it can participate in power dispatching. If the initial SOC is lower than 0.4, it needs to be charged immediately. The maximum SOC is 1, and the minimum SOC for the travel demand of users is 0.8. EV travel parameters are shown in Table I. The dispatching period of EVs is 5 min, the sampling points are 288, and the total time duration is 24 h.

TABLE I
SETTING OF TRAVEL PARAMETERS OF EVs

| Time | Number of EVs | Initial SOC | Arrival time | Depart time |
|---|---|---|---|---|
| 8:30–18:00 | 600 | N (0.65, 0.1) | N (9.3, 0.15) | N (17.5, 0.25) |
| 18:00–8:30 (2nd day) | 700 | N (0.4, 0.1) | N (18.5, 1.2) | N (7.5, 0.2) |

Figure 7(a) shows the sum of signals from the second branch of WPD to the penultimate branch in one day (the sampling interval is 5 min). If EVs are only used to suppress the above signals, then the demanded amount is shown in Fig. 7(b). We can see that the number of EVs required over the sample period is volatile.

According to the above analysis, we know that the schedulability of EVs is affected by multiple factors. Due to the mobility of EVs, we found that the supply of EVs is poor in two periods. In order to study the scheduling potential of EVs and maximize their role, we choose as many EVs as possible. By simulating the travel scenarios of EVs, the number of each time point under different samples can be obtained. Through multiple simulations, we finally selected a sample size of 1,300. The estimated number of EVs in the grid at each sampling point is shown in Fig. 8. We found that due to the uncertainty of EVs, they cannot be used as the



Fig. 5. Comparison of the original wind power with the grid-connected power.

### B. Results of Wind Power Stabilization Strategy

#### 1) Related Parameters of Energy Storage Equipment

In this study, the capacity of a single EV is 35 kWh, the charging power is 6.6 kW, the discharging power is −6.6 kW,
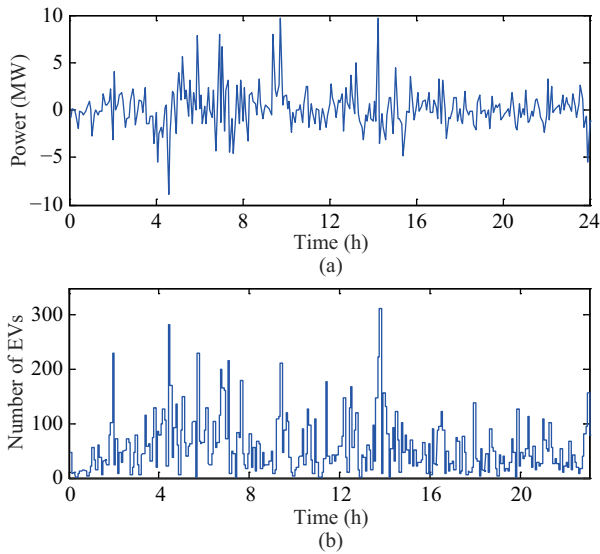
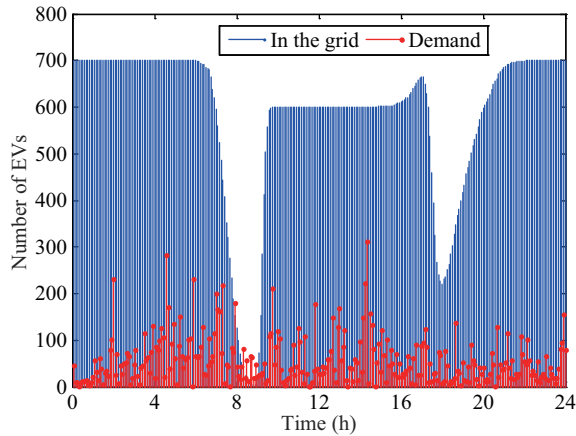Fig. 7.   Analysis of the demand for EVs.



Fig. 8.   Comparison of the actual quantity in the grid and the demand of EVs.

only energy storage equipment, other replenishment measures are needed to suppress wind power output fluctuations. From the previous analysis of WPD, the frequency of the last branch of the original output power is high. Thus, SC is selected for additional supply in this study. The capacity of the supercapacitor is set as 500 kWh. The rated charge and discharge power is 3 MW. The charge and discharge efficiency are 90%. The initial SOC is 0.6. The constraint range of SOC is 0.2–1.

*2) Analysis of Power Dispatching Results*

A large amount of statistics show that the cumulative value of the change in the number of charges and discharges of EVs is kept between 0 and 10, the dispatching potential value of EVs between 0 and 1, and the residual value of EVs in the power grid is generally around 100. Satisfactory weight coefficients can balance the three options above, and then focus on the dispatch flexibility of EVs. Through several simulations, we define the values of $\lambda$, $\alpha$ and $\beta$: 0.1, 1.5 and 0.001, respectively.

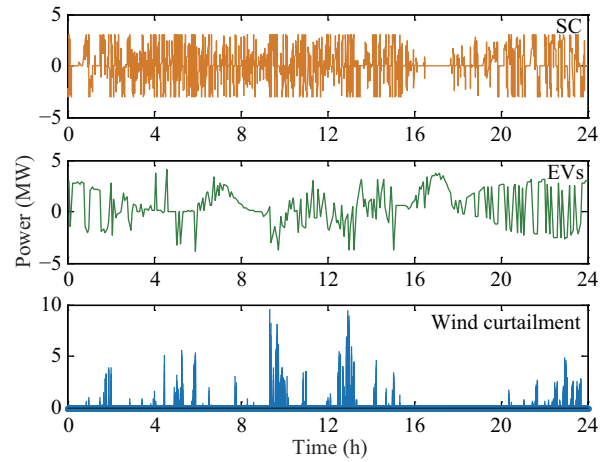Figure 9 shows that supercapacitors have fast response



Fig. 9.   Energy storage output power and wind curtailment.

speed and a large number of deep cycles. Their smoothing ability is good. The output power of the EV cluster is influenced by human factors. The smooth ability is poor from 8 am to 9 am and from 6 pm to 7 pm. The appropriate wind curtailment can be considered to obtain the target grid-connected power. When the curtailment quantity is at 2.51%, the actual grid-connected power can meet the constraints to the maximum extent. Given that EVs are greatly affected by the number of participating dispatches, we suggest the addition of other energy storage devices in the actual process of stabilizing fluctuations. The results may not be satisfactory when solely relying on EVs. Fig. 10 shows the variations of SOC of five EVs from arrival to departure in the grid. We can see that EVs guarantee user travel requirements and minimum dispatchable power.
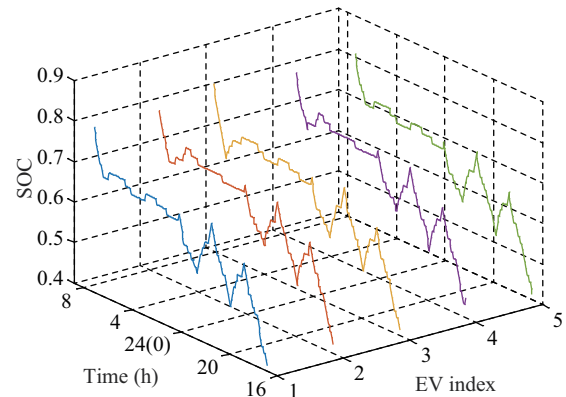


Fig. 10.   The variations of EV SOCs.

The comparison between the target grid-connected power and the actual grid-connected power is shown in Fig. 11. The correlation coefficient between the target grid-connected power and the actual grid-connected power is 0.998. This result verifies the effectiveness of the proposed strategy. In addition, we verified the target grid-connected power through Eq. (5), and found that it completely satisfies the fluctuation constraint conditions. Therefore, we believe that the research method in this paper can smooth the fluctuation of wind power
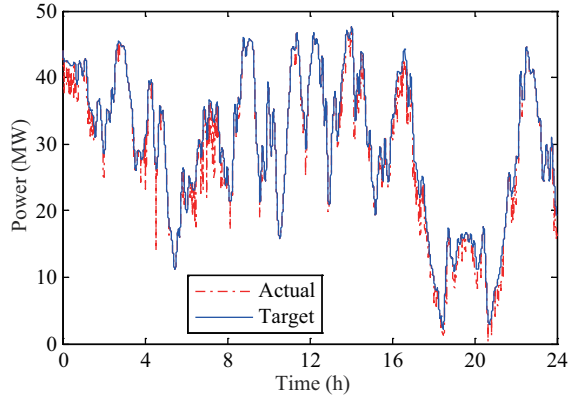
generation.



Fig. 11. Comparison of target and actual grid-connected power.

We contrasted the output of EVs calculated by DP using the traditional method and found that they vary. It can be seen from Table II and Fig. 12 that the energy storage replenishment capacity of EVs with KP is better, and the number of force charging marks are significantly lower than that with the traditional method. Through the above analysis, EVs with DP are considered highly capable.

TABLE II
COMPARISON OF STRATEGIES

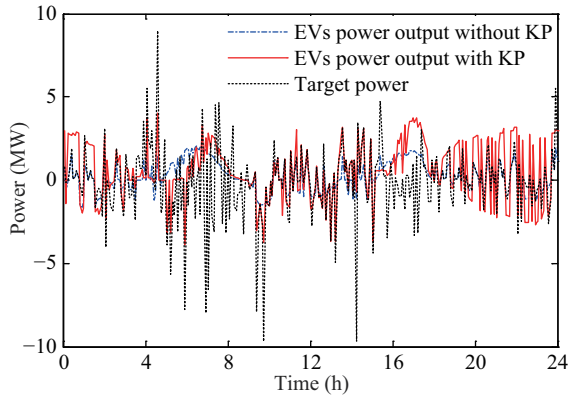| Method | Correlation coefficient | Forced charging |
|---|---|---|
| Method with KP | 0.60 | 10824 |
| Traditional method | 0.46 | 75800 |



Fig. 12. Comparison of the DP method for solving KP, the traditional method and the target smoothing deviation.

## V. CONCLUSION

Renewable energy that is directly connected to the grid will greatly harm the grid because of its high volatility. Only considering wind and solar curtailment to solve this problem will decrease economic benefits. Energy storage devices, such as EVs, have elastic power consumption time, bootable power consumption behavior, predictable power consumption, and intelligent power consumption patterns. We believe that a large space for load side resources can help in grid optimization

control. Therefore, the reasonable dispatching of EVs is of great significance. Research can be extended to study the bidirectional control between EVs and charging piles.

## REFERENCES

[1] P. Pinson, L. Mitridati, C. Ordoudis, and J. Østergaard, "Towards fully renewable energy systems: Experience and trends in Denmark, " *CSEE Journal of Power and Energy Systems*, vol. 3, no. 1, pp. 26–35, Mar. 2017.

[2] Y. B. Chen, Z. Zhang, Z. Y. Liu, P. Zhang, Q. Ding, X. Y. Liu, and W. R. Wang, "Robust $N - k$ CCUC model considering the fault outage probability of units and transmission lines," *IET Generation, Transmission & Distribution*, vol. 13, no. 17, pp. 3782–3791, Sep. 2019.

[3] Y. B. Chen, Z. Zhang, H. Chen, and H. P. Zheng, "Robust UC model based on multi-band uncertainty set considering the temporal correlation of wind/load prediction errors," *IET Generation, Transmission & Distribution*, vol. 14, no. 2, pp. 180–190, Jan. 2020.

[4] Y. B. Shu and Y. Tang, "Analysis and recommendations for the adaptability of China's power system security and stability relevant standards," *CSEE Journal of Power and Energy Systems*, vol. 3, no. 4, pp. 334–339, Dec. 2017.

[5] A. G. Olabi, "Renewable energy and energy storage systems," *Energy*, vol. 136, pp. 1–6, Oct. 2017.

[6] B. V. Mathiesen, H. Lund, D. Connolly, H. Wenzel, P. A. Østergaard, B. Möllerd, S. Nielsen, I. Ridjan, P. Karnøe, K. Sperling, and F. K. Hvelplund, "Smart energy systems for coherent 100% renewable energy and transport solutions," *Applied Energy*, vol. 145, pp. 139–154, May 2015.

[7] D. Larcher and J. M. Tarascon, "Towards greener and more sustainable batteries for electrical energy storage," *Nature Chemistry*, vol. 7, no. 1, pp. 19–29, 2015.

[8] M. Ding and J. Wu, "A novel control strategy of hybrid energy storage system for wind power smoothing," *Electric Power Components and Systems*, vol. 45, no. 12, pp. 1265–1274, Nov. 2017.

[9] F. Wu, J. Wang, Z. Sun, T. Wang, L. Chen, and X. Y. Han, "An optimal wavelet packets basis method for cascade hydro-PV-pumped storage generation systems to smooth photovoltaic power fluctuations," *Energies*, vol. 12, no. 24, pp. 4642, Dec. 2019.

[10] Q. Y. Jiang and H. S. Hong, "Wavelet-based capacity configuration and coordinated control of hybrid energy storage system for smoothing out wind power fluctuations," *IEEE Transactions on Power Systems*, vol. 28, no. 2, pp. 1363–1372, May 2013.

[11] K. C. Divya and J. Østergaard, "Battery energy storage technology for power systems-An overview," *Electric Power Systems Research*, vol. 79, no. 4, pp. 511–520, Apr. 2009.

[12] S. Hajiaghasi, A. Salemnia, and M. Hamzeh, "Hybrid energy storage system for microgrids applications: A review," *Journal of Energy Storage*, vol. 21, pp. 543–570, Feb. 2019.

[13] H. J. Jia, Y. F. Mu, and Y. Qi, "A statistical model to determine the capacity of battery-supercapacitor hybrid energy storage system in autonomous microgrid," *International Journal of Electrical Power & Energy Systems*, vol. 54, pp. 516–524, Jan. 2014.

[14] M. E. Choi, S. W. Kim, and S. W. Seo, "Energy management optimization in a battery/supercapacitor hybrid energy storage system," *IEEE Transactions on Smart Grid*, vol. 3, no. 1, pp. 463–472, Mar. 2012.

[15] L. Kouchachvili, W. Yaïci, and E. Entchev, "Hybrid battery/supercapacitor energy storage system for the electric vehicles," *Journal of Power Sources*, vol. 374, pp. 237–248, Jan. 2018.

[16] J. Huh, S. W. Lee, W. Y. Lee, G. H. Cho, and C. T. Rim, "Narrow-width inductive power transfer system for online electrical vehicles," *IEEE Transactions on Power Electronics*, vol. 26, no. 12, pp. 3666–3679, Dec. 2011.

[17] W. H. Hu, C. Su, Z. Chen, and B. Bak-Jensen, "Optimal operation of plug-in electric vehicles in power systems with high wind power penetrations," *IEEE Transactions on Sustainable Energy*, vol. 4, no. 3, pp. 577–585, Jul. 2013.

[18] H. Fathabadi, "Novel grid-connected solar/wind powered electric vehicle charging station with vehicle-to-grid technology," *Energy*, vol. 132, pp. 1–11, Aug. 2017.

[19] R. Loisel, G. Pasaoglu, and C. Thiel, "Large-scale deployment of electric vehicles in Germany by 2030: An analysis of grid-to-vehicle and vehicle-to-grid concepts," *Energy Policy*, vol. 65, pp. 432–443, Feb. 2014.

[20] Y. Cao, T. Wang, O. Kaiwartya, G. Y. Min, N. Ahmad, and A. H. Abdullah, "An EV charging management system concerning drivers' trip duration and mobility uncertainty," *IEEE Transactions on Systems, Man, and Cybernetics: Systems*, vol. 48, no. 4, pp. 596–607, Apr. 2018.

[21] J. Aghaei, A. E. Nezhad, A. Rabiee, and E. Rahimi, "Contribution of plug-in hybrid electric vehicles in power system uncertainty management," *Renewable and Sustainable Energy Reviews*, vol. 59, pp. 450–458, Jun. 2016.

[22] H. C. Zhang, Z. C. Hu, Z. W. Xu, and Y. H. Song, "Evaluation of achievable vehicle-to-grid capacity using aggregate PEV model," *IEEE Transactions on Power Systems*, vol. 32, no. 1, pp. 784–794, Jan. 2017.

[23] B. H. Qiao and J. Liu, "Multi-objective dynamic economic emission dispatch based on electric vehicles and wind power integrated system using differential evolution algorithm," *Renewable Energy*, vol. 154, pp. 316–336, Jul. 2020.

[24] X. Zhang, K. W. Chan, H. Z. Wang, B. Zhou, G. B. Wang, and J. Qiu, "Multiple group search optimization based on decomposition for multi-objective dispatch with electric vehicle and wind power uncertainties," *Applied Energy*, vol. 262, pp. 114507, Mar. 2020.

[25] C. H. Zheng, W. M. Li, and Q. Liang, "An energy management strategy of hybrid energy storage systems for electric vehicle applications," *IEEE Transactions on Sustainable Energy*, vol. 9, no. 4, pp. 1880–1888, Oct. 2018.

[26] S. Gao, K. T. Chau, C. H. Liu, D. Y. Wu, and C. C. Chan, "Integrated energy management of plug-in electric vehicles in power grid with renewables," *IEEE Transactions on Vehicular Technology*, vol. 63, no. 7, pp. 3019–3027, Sep. 2014.

[27] L. J. Zhang, X. M. Ye, X. H. Xia, and F. Barzegar, "A real-time energy management and speed controller for an electric vehicle powered by a hybrid energy storage system," *IEEE Transactions on Industrial Informatics*, vol. 16, no. 10, pp. 6272–6280, Oct. 2020.

[28] Q. Niu, K. C. Jiang, and Z. L. Yang, "An improved, negatively correlated search for solving the unit commitment problem's integration with electric vehicles," *Sustainability*, vol. 11, no. 24, pp. 6945, Dec. 2019.

[29] K. Seddig, P. Jochem, and W. Fichtner, "Integrating renewable energy sources by electric vehicle fleets under uncertainty," *Energy*, vol. 141, pp. 2145–2153, Dec. 2017.

[30] J. Y. Zhang, T. L. Shen, and J. Kako, "Short-term optimal energy management of power-split hybrid electric vehicles under velocity tracking control," *IEEE Transactions on Vehicular Technology*, vol. 69, no. 1, pp. 182–193, Jan. 2020.

[31] D. K. George and C. H. Xia, "Fleet-sizing and service availability for a vehicle rental system via closed queueing networks," *European Journal of Operational Research*, vol. 211, no. 1, pp. 198–207, May 2011.

[32] K. Kaur, A. Dua, A. Jindal, N. Kumar, M. Singh, and A. Vinel, "A novel resource reservation scheme for mobile PHEVs in V2G environment using game theoretical approach," *IEEE Transactions on Vehicular Technology*, vol. 64, no. 12, pp. 5653–5666, Dec. 2015.

[33] W. Zhou, L. Yang, Y. S. Cai, and T. X. Ying, "Dynamic programming for new energy vehicles based on their work modes part I: electric vehicles and hybrid electric vehicles," *Journal of Power Sources*, vol. 406, pp. 151–166, Dec. 2018.

[34] W. Zhou, L. Yang, Y. S. Cai, and T. X. Ying, "Dynamic programming for new energy vehicles based on their work modes Part II: Fuel cell electric vehicles," *Journal of Power Sources*, vol. 407, pp. 92–104, Dec. 2018.

[35] Y. S. Sun, Z. X. Zhao, M. Yang, D. Q. Jia, W. Pei, and B. Xu, "Overview of energy storage in renewable energy power fluctuation mitigation," *CSEE Journal of Power and Energy Systems*, vol. 6, no. 1, pp. 160–173, Mar. 2020.

[36] H. He, S. J. Cheng, Y. B. Zhang, and J. Nguimbis, "Home network power-line communication signal processing based on wavelet packet analysis," *IEEE Transactions on Power Delivery*, vol. 20, no. 3, pp. 1879–1885, Jul. 2005.

**Wei Wang** received the Ph.D. degree in Control Theory and Control Engineering from North China Electric Power University, Beijing, China, in 2011.

He is now an Associate Professor with the State Key Laboratory of Alternate Electrical Power System with Renewable Energy Sources, North China Electric Power University. His research interests include modeling, optimization and control of integrated energy system.
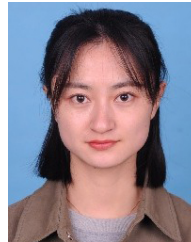
**Liu Liu** received the B.Sc. degree in Automation from North China Electric Power University, Baoding, China, in 2018.

She is currently pursuing her Ms. Degree in control theory and control engineering at North China Electric Power University, Beijing. Her research interests include modeling, optimization and control of integrated energy system.

**Jizhen Liu** received the Ms. Degree in Power Plant Engineering from the Graduate Faculty of North China Electric Power Institute, Beijing, China, in 1982.

He is now an academician with the China Engineering Academy, and a professor with the State Key Laboratory of Alternate Electrical Power System with Renewable Energy Sources, North China Electric Power University. His research interests include large-scale renewable energy integration.

**Zhe Chen** (M'95–SM'98–F'19) received the B.Eng. and M.Sc. degrees in Electrical Engineering from the Northeast China Institute of Electric Power Engineering, Jilin City, China, the M.Phil. degree in power electronics from Staffordshire University, Stoke-onTrent, U.K., and the Ph.D. degree in Electrical Engineering from the University of Durham, Durham, U.K. He is a Full Professor with the Department of Energy Technology, Aalborg University, Aalborg, Denmark. He is a Leader of the Wind Power System Research program with the Department of Energy Technology, Aalborg University and the Danish Principle Investigator for Wind Energy of the Sino-Danish Center for Education and Research. His research areas include power systems, power electronics and electric machines, and his main current research interests are wind energy and modern power systems. He has led many research projects and has more than 500 publications in his technical fields.